J|A|C|S COMMUNICATIONS

Published on Web 01/21/2009

Ultrasound-Induced Switching of Sheetlike Coordination Polymer Microparticles to Nanofibers Capable of Gelating Solvents

Shiyong Zhang, Shuaijun Yang, Jingbo Lan, Yurong Tang, Ying Xue, and Jingsong You*

Key Laboratory of Green Chemistry and Technology of Ministry of Education, College of Chemistry, and State Key Laboratory of Biotherapy, West China Hospital, Sichuan University, Chengdu 610064, People's Republic of China

Received October 25, 2008; E-mail: jsyou@scu.edu.cn

As a new class of hybrid inorganic−organic materials created by infinitely extending metal−ligand coordination interactions, crystalline coordination polymers have already shown promise in a broad range of applications, such as gas storage, molecular sieves, ion exchange, sensing, magnetism, and catalysis.[1] Recently, a rational design strategy based on the concept of coordination polymers toward supramolecular gels is starting to attract interest.[2,3] In particular, quite recent studies have demonstrated that the use of simple bridging organic units likewise facilitates the formation of coordination polymer gels in the absence of auxiliary moieties (e.g., hydroxy, cholesteryl, long hydrocarbon, ether chain, etc.) generally required, which offers new access to functional soft materials from structurally simple building blocks.[4]

Conventionally, supramolecular gels are prepared by heating a gelator in an appropriate solvent and subsequently cooling the resulting isotropic supersaturated solution to room temperature.[5] Since Naota and Koori observed ultrasound-triggered gelation for the first time,[6] the employment of sonication as an unexpected but effective stimulus to hydrogen bonding, $\pi-\pi$ stacking, and/or van der Waals interaction-dependent molecular gels has received unprecedented attention.[7] However, ultrasound-controllable supramolecular gels based on metal coordination interactions have been less explored, and to the best of our knowledge, only two examples are described so far. Rowan et al. reported a kind of metallo-supramolecular polymer gels exhibiting dramatic reversible responses to a variety of stimuli including sonication.[3d] Sijbesma et al. demonstrated reversible switching of the sol−gel transition *via* ultrasound-induced coordination polymer chain scission,[3b] which is assumed to change the network topology without changing the coordination chemistry.[8] In this communication, we wish to provide a new ultrasound-induced gelation mechanism with a modification of the coordination mode of coordination polymers.

Although there is extensive literature on the synthesis and characterization of bulk coordination polymer materials, few reports have appeared on coordination polymer micro- or nanoparticles (CPPs).[9] We herein demonstrate a new class of micrometer-scale sheetlike CPPs $\{Zn(bibp)_2(OSO_2CF_3)_2\}_n$ (**1**) constructed by $Zn(OSO_2CF_3)_2$ and 4,4′-bis(1-imidazolyl)biphenyl (bibp). More interestingly, as the CPPs were subjected to irradiation with ultrasound, a dramatic morphological transformation was observed from sheetlike microparticles to nanofibers, which further entangled each other to form a three-dimensional fibrillar network thereby resulting in the immobilization of organic fluids (Scheme 1). This is a completely new phenomenon observed for coordination polymers.

Coordination polymer particles $\{Zn(bibp)_2(OSO_2CF_3)_2\}_n$ (**1**) were prepared as follows: A methanol solution of $Zn(OSO_2CF_3)_2$ was added to a methanol solution of 4,4′-bisimidazolylbiphenyl (bibp) in a 1:2 molecular ratio with vigorous stirring at room temperature to yield a white suspension, followed by being left to stand for 24 h.[10] The precipitate formed was collected by centrifugation and washed several times with water and methanol. The scanning electron micrographic (SEM) image of **1** redispersed in methanol revealed the formation of sheetlike microparticles with uniform shape and size (Figure 1). The chemical composition of the CPPs was further characterized by ^1H and ^{13}C NMR spectra, TGA, ICP, and elemental analysis, which are in full agreement with the chemical structure presented (see Supporting Information).

Scheme 1

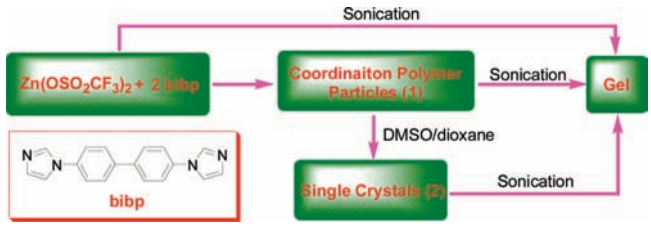

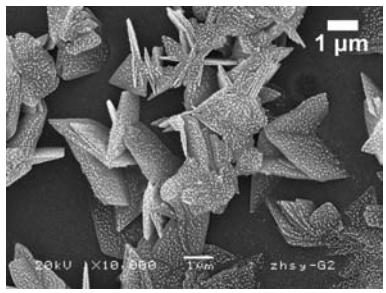

Figure 1. SEM photograph of sheetlike microparticles of $\{Zn(bibp)_2(OSO_2CF_3)_2\}_n$ (**1**), Au shadowing at 45°. The small white dots are the gold aggregates.

After numerous attempts, luckily, colorless block crystals of $\{Zn(bibp)_2(OSO_2CF_3)_2 \cdot (DMSO)_x \cdot (dioxane)_y \cdot (H_2O)_z\}_n$ (**2**) were obtained by slow diffusion of dioxane into a solution of **1** in dimethyl sulfoxide (DMSO) in a thermostat (40 °C) for ∼2 months.[11,12] The asymmetric unit of **2** shows that the Zn(II) adopts a tetrahedron coordination geometry (Figure 2a). Every zinc ion is coordinated by four imidazole nitrogen atoms from four different bibp molecules, whose other nitrogens serve as bridging positions to connect the adjacent identical zinc(II), leading to the formation of 2-D layers with extraordinarily big square cavities (17.9 × 17.5 Å^2, Figure 2b, and also see Figure S4). The trifluoromethanesulfonate ($CF_3SO_3^-$) anions do not participate in the coordination but act as counteranions located in the squares. Very interestingly, the 2-D networks, despite arranging in an offset way, are stacked along the crystallographic *a* axis to create two kinds of large one-dimensional channels **A** and **B**, which have internal van der Waals dimensions of ∼17 × 9 Å^2 and 9 × 9 Å^2, respectively (Figure 2c).

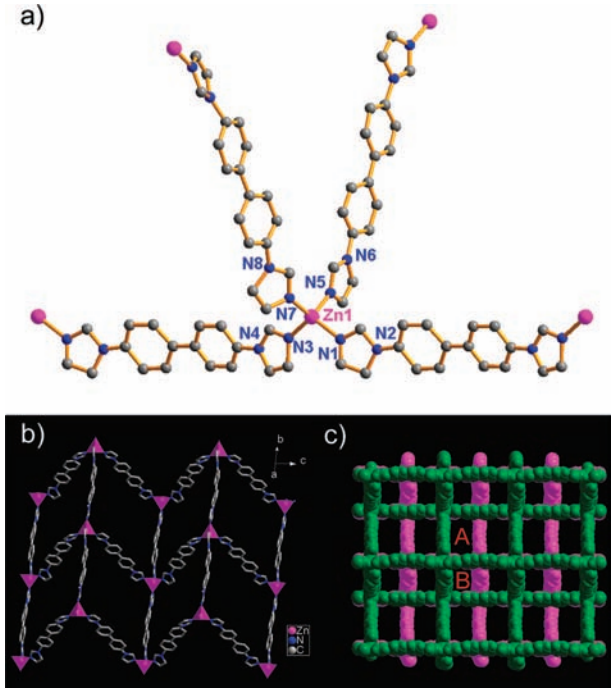

Figure 2. (a) Coordination mode of zinc atom of **2**. All hydrogen atoms and solvent molecules as well as uncoordinated $CF_3SO_3^-$ anions were omitted for clarity. (b) Infinite 2D layer of **2**. The pink polyhedrons represent coordination geometry of zinc(II). (c) Space-filling projection showing the packing arrangement of **2** host complexes to form two large rectangular channels along *a* axis (channel **A**: *ca.* 17 × 9 Å^2; channel **B**: *ca.* 9 × 9 Å^2). Alternate layers are represented by identical colors.

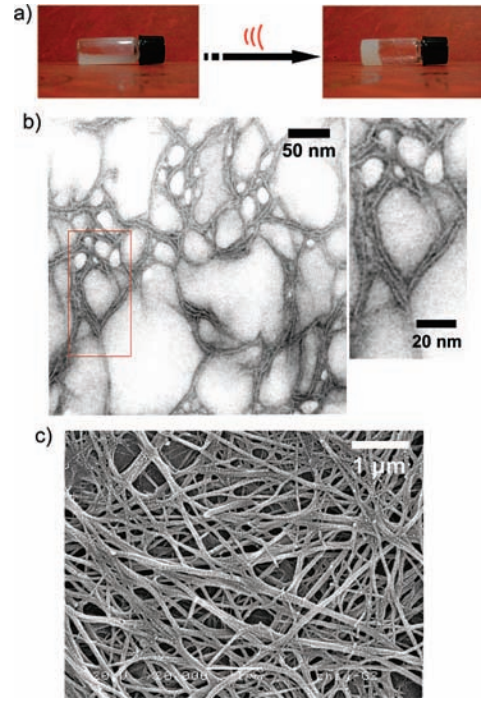

Figure 3. (a) Coordination polymer **1** in methanol: a suspension before sonication (left), and a gel after sonication (right). (b) TEM image obtained from the gel of **1** in methanol, 2.0 wt%, negatively stained with uranyl acetate aqueous solution. The inset (right) shows a zoomed-in image marked in b, which indicates the nanofibers have a diameter of *ca*. 3.0−4.0 nm. (c) SEM picture of xerogel obtained from the gel of **1** in methanol, 2.0 wt%, Au shadowing at 45°.

Both **A** and **B** are occupied by disordered solvent molecules. Somewhat regrettably, we were unable to establish an unambiguous correlation between the structure of **2**, as determined by single-crystal X-ray diffraction, and that of the CPPs **1**, as revealed by studies using powder X-ray diffraction (Figure S5), presumably due to partial collapse of the crystal lattice of **1** in the absence of solvent molecules.

The sheetlike microparticles **1** were not soluble in methanol but gave rise to a white suspension even at elevated temperatures. Interestingly, as the suspension was submitted to sonication (0.45 W/cm^2, 40 KHz) for a period of 1−3 min, a complete and homogeneous liquid gelation was observed (Figure 3a). This opaque white gel that formed could be stable for months at room temperature without visible changes. Gelation also proceeded well in ethanol and acetonitrile by ultrasonic treatment (Table S1). In the case of acetonitrile, 1 g of $\{Zn(bibp)_2(OSO_2CF_3)_2\}_n$ (**1**) was capable of immobilizing 125 g of solvent (critical gel concentration = 0.8 wt%), and **1** may be considered as a "supergelator" accordingly.[13] Furthermore, the sol−gel phase transition temperature (T_{gel}) of **1** in methanol, ethanol, and acetonitrile exceeded the boiling points of the solvents, and boiling only occurred upon decomposition of the gels (boiling at T_{gel}, Table S2). It should be noted that both the crystal sample of **2** and in situ mixing of $Zn(OSO_2CF_3)_2$ and bibp could likewise gelate the organic fluids with sonication (Scheme 1).

High resolution transmission electron microscopy (TEM) clearly revealed the supramolecular structure of the gels. To our surprise, the morphologies of samples did become quite different after ultrasound. As shown in Figure 3b, the TEM image obtained from the gel of $\{Zn(bibp)_2(OSO_2CF_3)_2\}_n$ (**1**) in methanol indicated the presence of well-grown distinct fibrillar assemblies with a uniform diameter of ∼3.0−4.0 nm and lengths up to several micrometers,[14] which is responsible for gelation. In addition, a typical SEM micrograph, obtained from the freeze-dried gel (xerogel) by sonication in methanol, also demonstrated the formation of well-developed three-dimensional networks composed of interlocked fibers with a diameter of 50−200 nm, which should be aggregated by nanofibers during the drying process (Figure 3c).[15]

The powder X-ray diffraction pattern of the xerogels showed a high degree of noncrystallinity which prevents a detailed analysis of the structural connectivity of the fibers (Figure S5). Nevertheless, the CP/MAS solid-state ^{13}C NMR spectroscopic experiments of samples provided additional short-range information regarding the environment of the metal ions before and after sonication. As shown in Figure 4a, the aromatic carbon peaks of microparticles appeared from 114.13 to 139.03 ppm. After sonication, the peak at 114.13 ppm disappeared. Concomitantly, the signals at 139.03 and 121.39 ppm shifted upfield to 138.32 and 120.87 ppm, respectively (Figure 4b). These results are indicative of the difference of the coordination environment of the metal ions between the CPPs and xerogels.

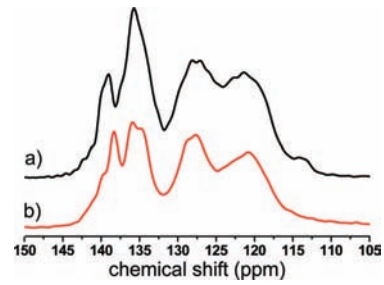

Figure 4. Comparison of CP/MAS solid-state ^{13}C NMR spectra of microparticles (a) and xerogels (b).

Considering the length of rigid bibp (14.1 Å estimated by the crystal structure of bibp·H_2O,[11] Figures S6 and S7) and the coordination geometry of zinc(II) as well as the ratio of metal ion and ligand, a possible mode of the nanofibers observed above was proposed (Figure 5a),[16] in which the zinc(II) ions show a coordination geometry toward the organic ligands that is not the tetrahedron but the seesaw (Figure 5b). Although in this mode the Zn ions should exhibit some tension on the metal center, we believe that this can form when ultrasound is applied.[17] In other words, sonication was assumed to facilitate a break−reorganization of coordination bonds, which led to the morphological transition from sheetlike microparticles to nanofibers capable of gelating solvents. It should be notable that the formation of coordination polymer gels *via* thermochromic[3h] and anion-triggered[3f] coordination structure changes has ever been discussed. However, as far as we know, there are not examples describing the generation of coordination polymer gels *via* a sonication-induced coordination geometry modification.

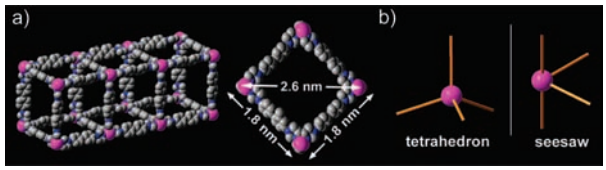

Figure 5. (a) A proposed mode of the nanofibers, visualized by GaussView 3.07. Pink, Zn; cyan, N; gray, C. All $CF_3SO_3^-$ ions and H atoms were omitted for clarity. (b) Coordination mode of Zn ions: tetrahedron before sonication (left); seesaw after soincation (right).

In conclusion, we have described ultrasound-induced switching of sheetlike coordination polymer microparticles to nanofibers capable of gelating a variety of organic solvents. The experimental results indicate that the gelation is most likely to originate from the change of coordination chemistry of metal ions driven by sonication. Efforts are now in progress to investigate the full scope of the transformation to obtain a detailed mechanism and to apply this method to other coordination polymer systems.

Acknowledgment. This work was supported by grants from the National NSF of China (Nos. 20772086, 20602027, and 20572074). We thank the Centre of Testing & Analysis, Sichuan University for X-ray crystallographic, TEM, SEM, and NMR measurements. We are also grateful to Prof. Guangshan Zhu (Jilin University) for helpful discussions.

Supporting Information Available: Experimental procedures, analytical data, 7 figures, 3 tables, and crystallographic data of bibp·H_2O and **2** (CIF). This material is available free of charge via the Internet at http://pubs.acs.org.

References

(1) Lehn, J.-M. *Supramolecular Chemistry: Concepts and Perspectives*; VCH: Weinheim, 1995. (b) Férey, G.; Mellot-Draznieks, C.; Serre, C.; Millange, F. *Acc. Chem. Res.* **2005**, *38*, 217. (c) Hupp, J. T.; Poeppelmeier, K. R. *Science* **2005**, *309*, 2008. (d) Kitagawa, S.; Kitaura, R.; Noro, S. *Angew. Chem., Int. Ed.* **2004**, *43*, 2334. (e) Yaghi, O. M.; O'Keeffe, M.; Ockwig, N. W.; Chae, H. K.; Eddaoudi, M.; Kim, J. *Nature* **2003**, *423*, 705. (f) Forster, P. M.; Cheetham, A. K. *Top. Catal.* **2003**, *24*, 79.

(2) A highlight article describing coordination chemistry as a rational design route toward gels, see: Fages, F. *Angew. Chem., Int. Ed.* **2006**, *45*, 1680.

(3) For selected examples of coordination polymer gels, see: (a) Leong, W. L.; Tam, A. Y.-Y.; Batabyal, S. K.; Koh, L. W.; Kasapis, S.; Yam, V. W.-W.; Vittal, J. J. *Chem. Commun.* **2008**, 3628. (b) Paulusse, J. M. J.; van Beek, D. J. M.; Sijbesma, R. P. *J. Am. Chem. Soc.* **2007**, *129*, 2392. (c) Hui, J. K.-H.; Yu, Z.; MacLachlan, M. J. *Angew. Chem., Int. Ed.* **2007**, *46*, 7980. (d) Weng, W.; Beck, J. B.; Jamieson, A. M.; Rowan, S. J. *J. Am. Chem. Soc.* **2006**, *128*, 11663. (e) Beck, J. B.; Rowan, S. J. *J. Am. Chem. Soc.* **2003**, *125*, 13922. (f) Kim, H.-J.; Lee, J.-H.; Lee, M. *Angew. Chem., Int. Ed.* **2005**, *44*, 5810. (g) Kim, H.-J.; Zin, W.-C.; Lee, M. *J. Am. Chem. Soc.* **2004**, *126*, 7009. (h) Kuroiwa, K.; Shibata, T.; Takada, A.; Nemoto, N.; Kimizuka, N. *J. Am. Chem. Soc.* **2004**, *126*, 2016. (i) Roubeau, O.; Colin, A.; Schmitt, V.; Clérac, R. *Angew. Chem., Int. Ed.* **2004**, *43*, 3283. (j) Xing, B.; Choi, M.-F.; Xu, B. *Chem.—Eur. J.* **2002**, *8*, 5028. (k) Xing, B.; Choi, M.-F.; Xu, B. *Chem. Commun.* **2002**, 362.

(4) Zhang, S.; Yang, S.; Lan, J.; Yang, S.; You, J. *Chem. Commun.* **2008**, 6170.

(5) (a) George, M.; Weiss, R. G. *Acc. Chem. Res.* **2006**, *39*, 489. (b) Sangeetha, N. M.; Maitra, U. *Chem. Soc. Rev.* **2005**, *34*, 821. (c) Estroff, L. A.; Hamilton, A. D. *Chem. Rev.* **2004**, *104*, 1201. (d) Van Bommel, K. J. C.; Friggeri, A.; Shinkai, S. *Angew. Chem., Int. Ed.* **2003**, *42*, 980.

(6) Naota, T.; Koori, H. *J. Am. Chem. Soc.* **2005**, *127*, 9324.

(7) For selected examples, see: (a) Bardelang, D.; Camerel, F.; Margeson, J. C.; Leek, D. M.; Schmutz, M.; Zaman, M. B.; Yu, K.; Soldatov, D. V.; Ziessel, R.; Ratcliffe, C. I.; Ripmeester, J. A. *J. Am. Chem. Soc.* **2008**, *130*, 3313. (b) Wu, J.; Yi, T.; Shu, T.; Yu, M.; Zhou, Z.; Xu, M.; Zhou, Y.; Zhang, H.; Han, J.; Li, F.; Huang, C. *Angew. Chem., Int. Ed.* **2008**, *47*, 1063. (c) Anderson, K. M.; Day, G. M.; Paterson, M. J.; Byrne, P.; Clarke, N.; Steed, J. W. *Angew. Chem., Int. Ed.* **2008**, *47*, 1058. (d) Liu, J.; He, P.; Yan, J.; Fang, X.; Peng, J.; Liu, K.; Fang, Y. *Adv. Mater.* **2008**, *20*, 2508. (e) Baddeley, C.; Yan, Z.; King, G.; Woodward, P. M.; Badjić, J. D. *J. Org. Chem.* **2007**, *72*, 7270. (f) Isozaki, K.; Takaya, H.; Naota, T. *Angew. Chem., Int. Ed.* **2007**, *46*, 2855. (g) Paulusse, J. M. J.; Sijbesma, R. P. *Angew. Chem., Int. Ed.* **2006**, *45*, 2334. (h) Wang, C.; Zhang, D.; Zhu, D. *J. Am. Chem. Soc.* **2005**, *127*, 16372.

(8) (a) Paulusse, J. M. J.; Huijbers, J. P. J.; Sijbesma, R. P. *Chem.—Eur. J.* **2006**, *12*, 4928. (b) Paulusse, J. M. J.; Sijbesma, R. P. *Angew. Chem., Int. Ed.* **2004**, *43*, 4460.

(9) (a) Jung, S.; Oh, M. *Angew. Chem., Int. Ed.* **2008**, *47*, 2049. (b) Imaz, I.; Maspoch, D.; Rodrı´guez-Blanco, C.; Pérez-Falcón, J. M.; Campo, J.; Ruiz-Molina, D. *Angew. Chem., Int. Ed.* **2008**, *47*, 1857. (c) Jeon, Y.-M.; Armatas, G. S.; Heo, J.; Kanatzidis, M. G.; Mirkin, C. A. *Adv. Mater.* **2008**, *20*, 2105. (d) Jeon, Y.-M.; Heo, J.; Mirkin, C. A. *J. Am. Chem. Soc.* **2007**, *129*, 7480. (e) Maeda, H.; Hasegawa, M.; Hashimoto, T.; Kakimoto, T.; Nishio, S.; Nakanishi, T. *J. Am. Chem. Soc.* **2006**, *128*, 10024. (f) Rieter, W. J.; Taylor, K. M. L.; An, H.; Lin, W.; Lin, W. *J. Am. Chem. Soc.* **2006**, *128*, 9024. (g) Würthner, F.; Stepanenko, V.; Sautter, A. *Angew. Chem., Int. Ed.* **2006**, *45*, 1939. (h) Oh, M.; Mirkin, C. A. *Nature* **2005**, *438*, 651. (i) Sun, X.; Dong, S.; Wang, E. *J. Am. Chem. Soc.* **2005**, *127*, 13102.

(10) For preparation of bibp, see: Zhang, S.; Lan, J.; Mao, Z.; Xie, R.; You, J. *Cryst. Growth Des.* **2008**, *9*, 3134.

(11) For crystallographic data, see: Supporting Information, Table S3.

(12) The exact number of guest molecules in the crystallographic asymmetry unit can not be determined according to the Fourier electron densities due to disorder. However, the host framework can be located exactly.

(13) (a) Klawonn, T.; Gansäuer, A.; Winkler, I.; Lauterbach, T.; Franke, D.; Nolte, R. J. M.; Feiters, M. C.; Börner, H.; Hentschelc, J.; Dötz, K. H. *Chem. Commun.* **2007**, 1894. (b) Murata, K.; Aoki, M.; Suzuki, T.; Harada, T.; Kawabata, H.; Komori, T.; Ohseto, F.; Ueda, K.; Shinkai, S. *J. Am. Chem. Soc.* **1994**, *116*, 6664.

(14) To obtain the clear TEM images of high resolution, the negative staining was adopted to provide contrast, while without staining no distinguishable structures were visible. The darker contrast in the outer region of the fibers should partially come from the inorganic staining. Therefore, although these fibers resemble tubes, we could not provide further technique to support their presence at this stage.

(15) Sometimes micrometer-scale sheets were not completely transferred to fibers and could be observed from the xerogels accordingly.

(16) The size of the proposed nanofibers is slightly lower than that observed in TEM experiments (*ca.* 3.0−4.0 nm). This difference could be easily explained by the negative staining, which makes the size of the fibers observed slightly higher than that of its real structure due to the coating of the contrasting reagent around the periphery of the fibers. While deducting the darker contrast in the outer region, a lighter region in the center of the observed fibers is ca. 1.5−2.2 nm, considered as the internal dimensions, which is roughly consistent with that of the proposed mode.

(17) Metal−ligand interactions not only are thermodynamically stable but also, depending on the metal ion and ligand used, can be kinetically labile. For a related description, see: (a) Kurth, D. G.; Higuchi, M. *Soft Matter* **2006**, *2*, 915. (b) Yount, W. C.; Loveless, D. M.; Craig, S. L. *J. Am. Chem. Soc.* **2005**, *127*, 14488. (c) Loveless, D. M.; Jeon, S. L.; Craig, S. L. *Macromolecules* **2005**, *38*, 10171. (d) Yount, W. C.; Juwarker, H.; Craig, S. L. *J. Am. Chem. Soc.* **2003**, *125*, 15302.

JA808210Z